Supplementary material

Tunable Schottky contacts in graphene/XAu_4Y (X, Y = Se, Te) heterostructures

Yufei Xue[†,#], Lei Gao[†,‡,#,*], Weina Ren[†], Xuxia Shai[†], Tingting Wei[†], Chunhua Zeng[†,*], Hua Wang[‡,*]

[†] Institute of Physical and Engineering Science/Faculty of Science, Kunming University of Science and Technology, Kunming 650500, Yunnan, China

[‡] State Key Laboratory of Complex Nonferrous Metal Resources Clean Utilization, Kunming University of Science and Technology, Kunming 650093, Yunnan, China

[#] These authors contributed equally.

[*] Corresponding author.

E-mail: lgao@kust.edu.cn (Lei Gao); chzeng83@kust.edu.cn (Chunhua Zeng); wanghua65@163.com (Hua Wang)

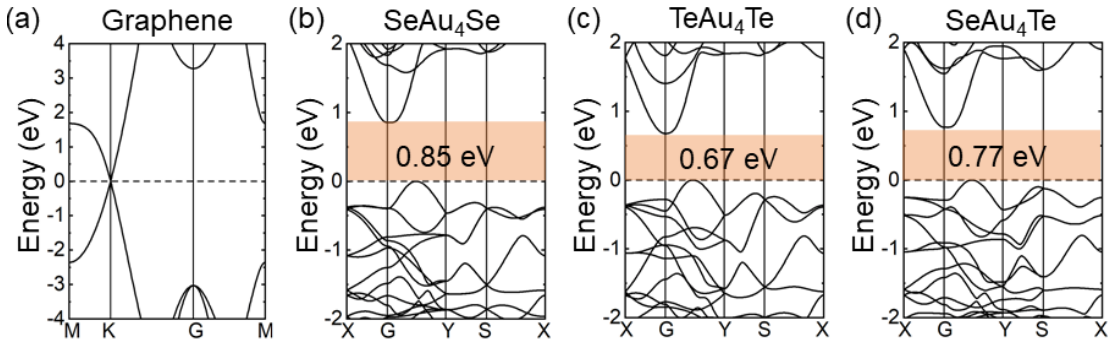

Figure S1 Energy band structures of (a) graphene, (b) $SeAu_4Se$, (c) $TeAu_4Te$ and (d) $SeAu_4Te$ monolayers, respectively.

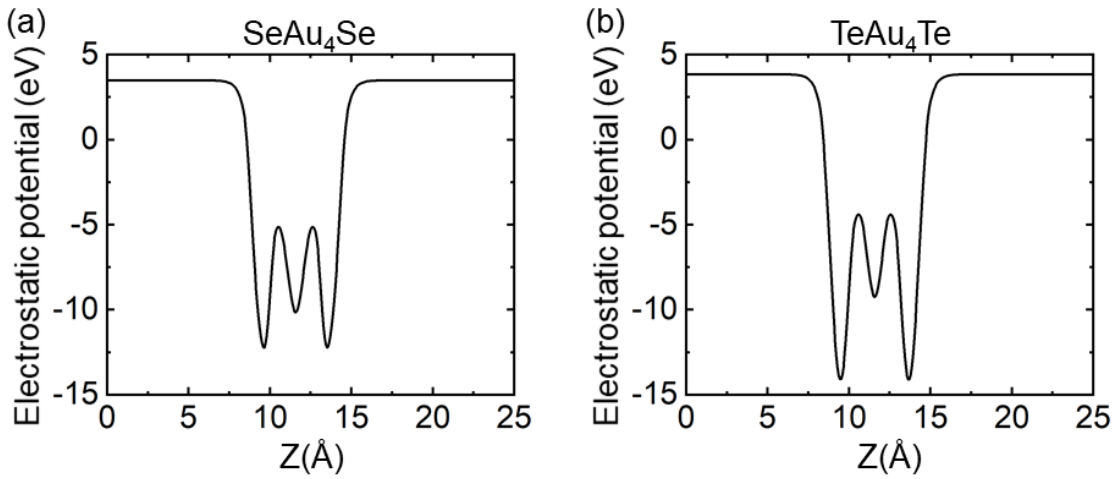

Figure S2 Electrostatic potentials of (a) $SeAu_4Se$ and (b) $TeAu_4Te$ monolayers, respectively.

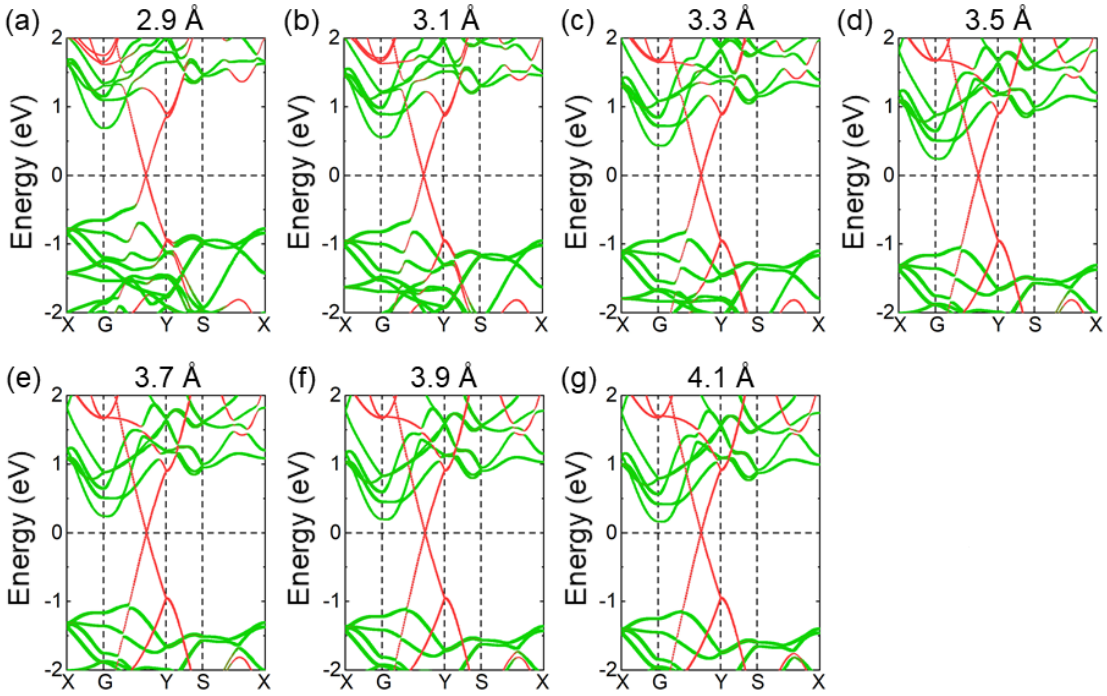

Figure S3 (a)-(g) Projected band structures of G/$SeAu_4Se$ heterostructure with different interlayer distances. The contributions of G and $SeAu_4Se$ monolayers are marked by red and green, respectively.

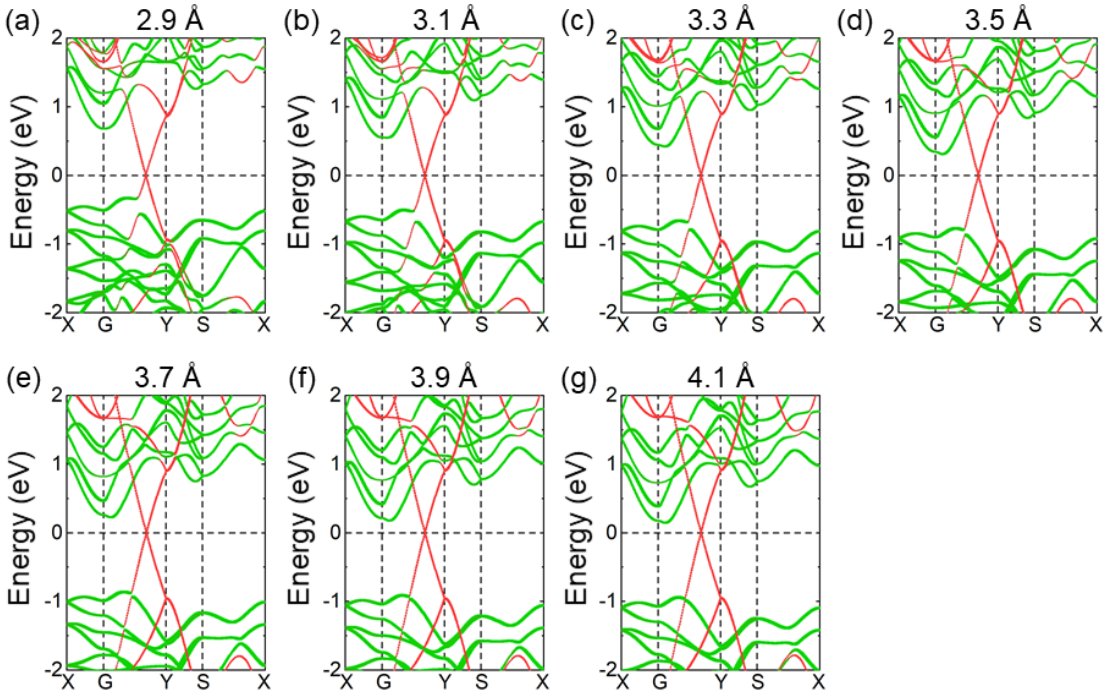

Figure S4 (a)-(g) Projected band structures of G/$SeAu_4Te$ heterostructure with different interlayer distances. The contributions of G and $SeAu_4Te$ monolayers are marked by red and green, respectively.

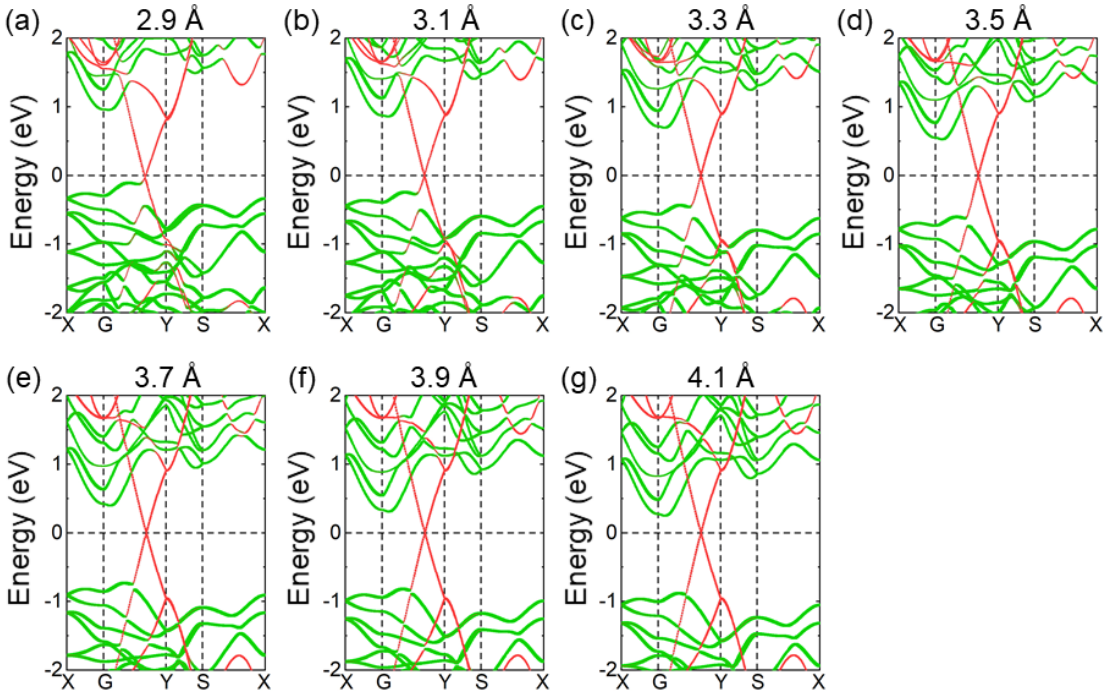

Figure S5 (a)-(g) Projected band structures of G/$TeAu_4Se$ heterostructure with different interlayer distances. The contributions of G and $TeAu_4Se$ monolayers are marked by red and green, respectively.

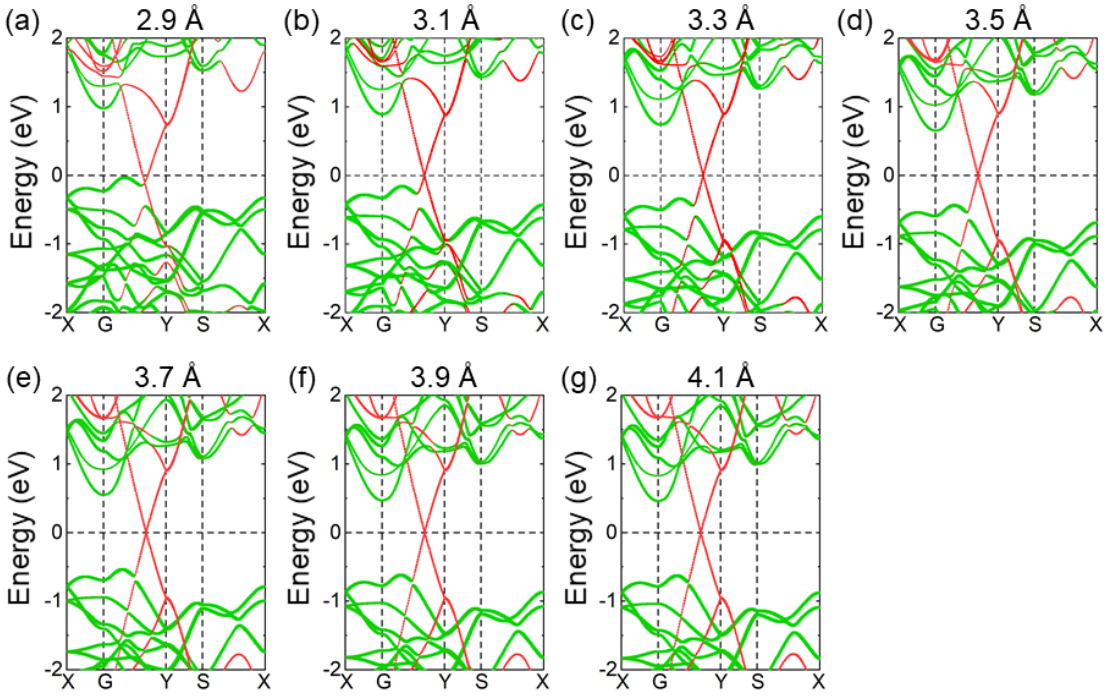

Figure S6 (a)-(g) Projected band structures of G/$TeAu_4Te$ heterostructures with different interlayer distances. The contributions of G and $TeAu_4Te$ monolayers are marked by red and green, respectively.

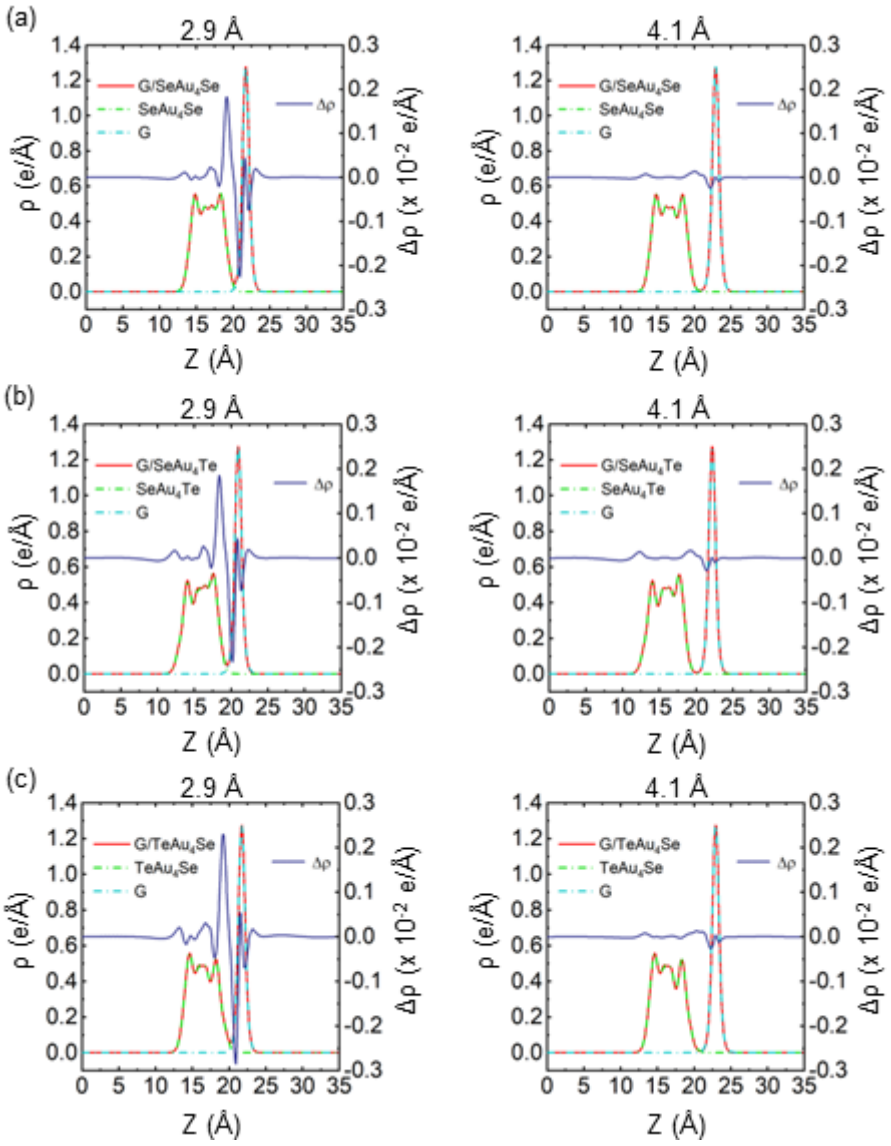

Figure S7 Charge density differences of (a) G/$SeAu_4Se$, (b) G/$SeAu_4Te$ and (c) G/$TeAu_4Se$ heterostructures with interlayer distances of 2.9 and 4.1 Å. The charge density difference of heterostructures is denoted by blue solid line. The charge densities of G/XAu_4Y, G and XAu_4Y are denoted by red solid lines, cyan and green dotted lines, respectively.

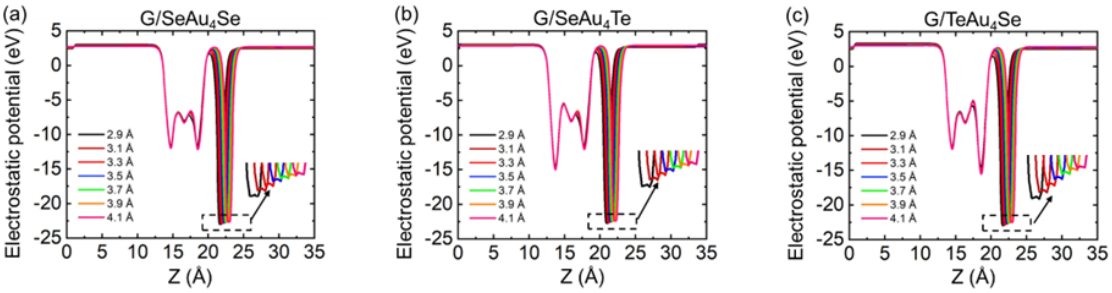

Figure S8 Electrostatic potentials of (a) G/$SeAu_4Se$, (b) G/$SeAu_4Te$ and (c) G/$TeAu_4Se$ heterostructures with interlayer distances from 2.9 to 4.1 Å. With the interlayer distance decreasing, the amount of transferred electrons increases, and meanwhile, the potential well of G notably becomes deeper, leading to a stronger interfacial electrostatic field.

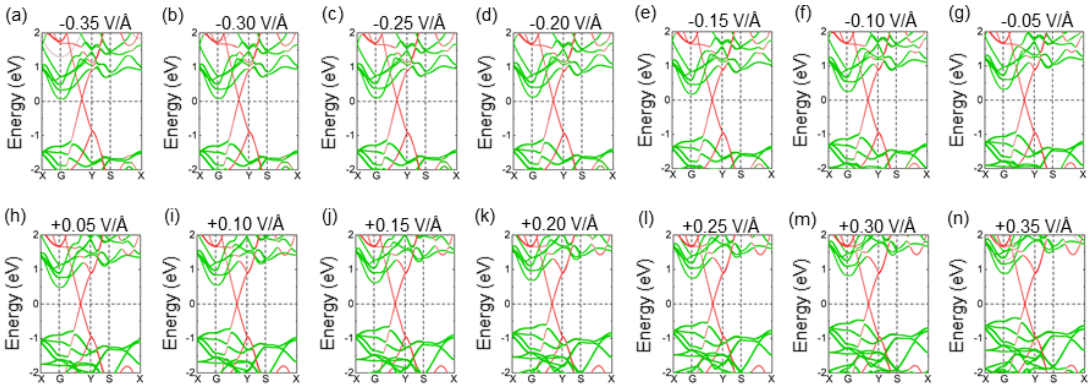

Figure S9 (a)-(n) Projected band structures of G/$SeAu_4Se$ heterostructures with -0.35 to +0.35 V/Å electric fields. The contributions of G and $SeAu_4Se$ monolayers are marked by red and green, respectively.

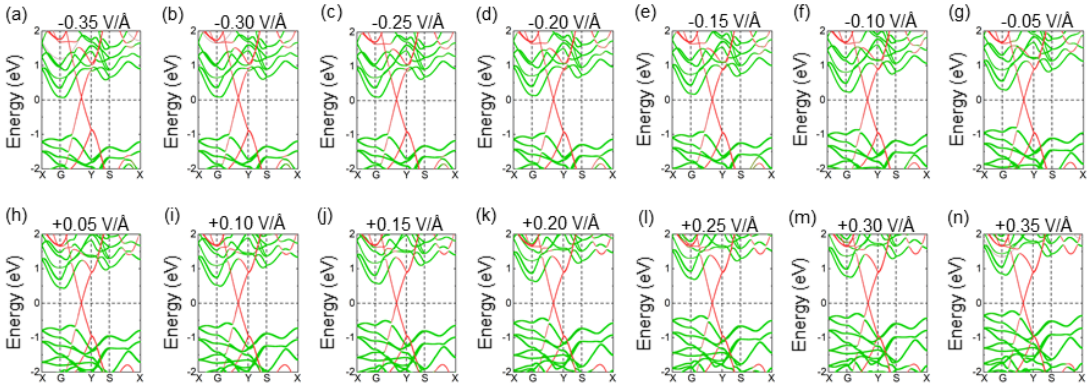

Figure S10 (a)-(n) Projected band structures of G/$SeAu_4Te$ heterostructures with -0.35 to +0.35 V/Å electric fields. The contributions of G and $SeAu_4Te$ monolayers are marked by red and green, respectively.

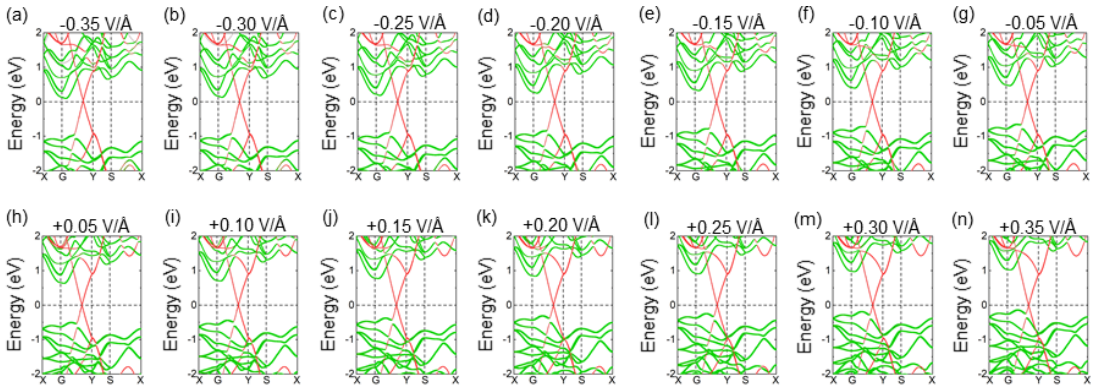

Figure S11 (a)-(n) Projected band structures of G/$TeAu_4Se$ heterostructures with -0.35 to +0.35 V/Å electric fields. The contributions of G and $TeAu_4Se$ monolayers are marked by red and green, respectively.

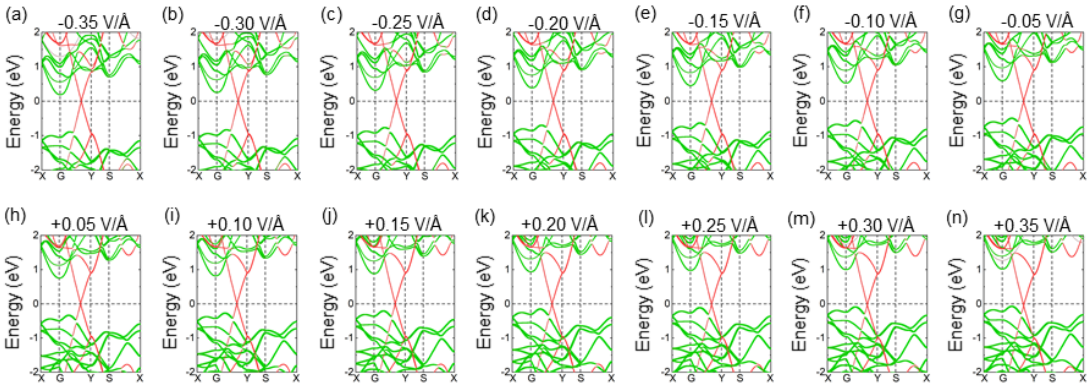

Figure S12 (a)-(n) Projected band structures of G/$TeAu_4Te$ heterostructures with -0.35 to +0.35 V/Å electric fields. The contributions of G and $TeAu_4Te$ monolayers are marked by red and green, respectively.

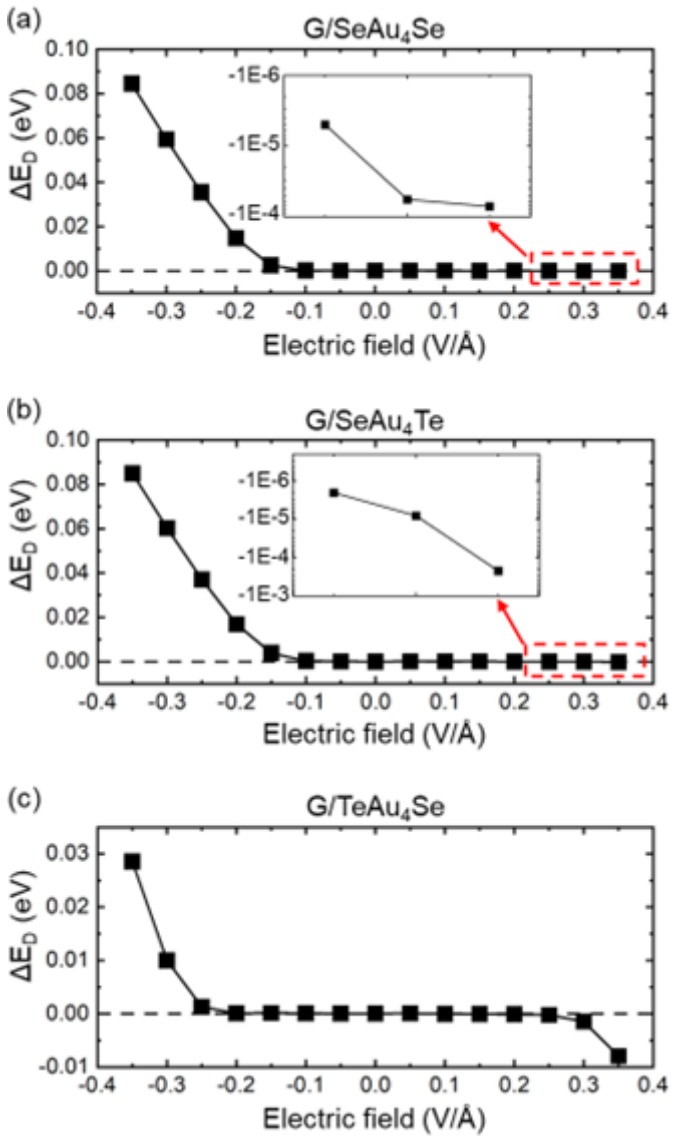

Figure S13 Energy shift of graphene's Dirac cone with respect to the Fermi level for (a) $G/SeAu_4Se$, (b) $G/SeAu_4Te$ and (c) $G/TeAu_4Se$ as a function of electric field from -0.35 to +0.35 V/Å.

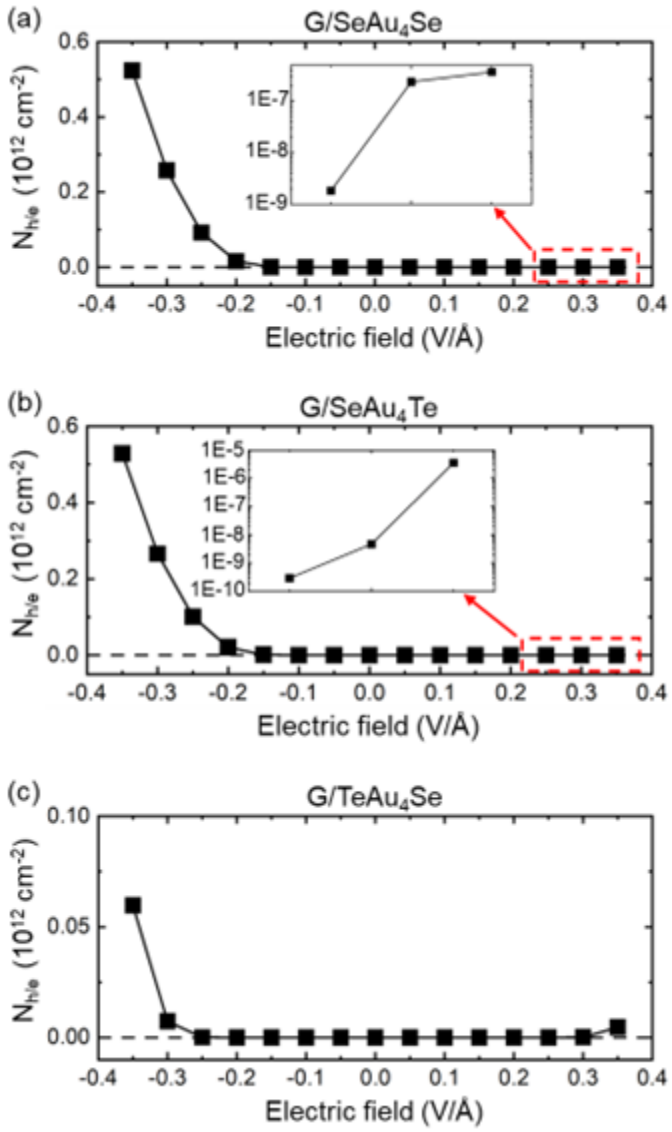

Figure S14 Doping charge carrier concentrations of graphene in (a) $G/SeAu_4Se$, (b) $G/SeAu_4Te$ and (c) $G/TeAu_4Se$ as a function of electric field from -0.35 to +0.35 V/Å. The hole (electron) doping charge carrier concentrations of graphene correspond to $\Delta E_D>0$ ($\Delta E_D<0$) in figure S13.

Table S1 The structural parameters and dipole moments of $SeAu_4Se$, $TeAu_4Te$, $SeAu_4Te$ monolayers, respectively.

Monolayer	*a* (Å)	*b* (Å)	Dipole moments (Debye)
$SeAu_4Se$	7.54	5.25	0.00
$TeAu_4Te$	7.92	5.36	0.00
$SeAu_4Te$	7.72	5.31	0.22